The Effect of CO on Hydrogen Permeation through Pd and Internally Oxidized and Un-oxidized Pd Alloy Membranes.

Ted B.Flanagan*, D. Wang* and Kirk Shanahan*,*,
*Material Science Program and Department of Chemistry,
University of Vermont,
Burlington VT 05405 USA,
, Savannah River National Laboratory, Aiken, S.C. 29808

Abstract

The H permeation of internally oxidized Pd alloy membranes such as *Pd*–Al and *Pd*–Fe, but not *Pd*–Y alloys, is shown to be more resistant to inhibition by CO(g) as compared to Pd or un-oxidized Pd alloy membranes. The increased resistance to CO is found to be greater at 423 K than at 473 K or 523 K. In these experiments CO was pre-adsorbed onto the membranes and then CO-free H_2 was introduced to initiate the H permeation.

Introduction

It has been found [1] for H permeation through Pd-based membranes that partially internally oxidized (IOed) *Pd*–Al alloys have a greater resistance to CO inhibition than Pd or un-oxidized *Pd*–Al alloys. It was also found earlier by the present workers [1] that the degree of CO inhibition increases as the flux increases and therefore a comparison of the CO inhibition of an IOed alloy with Pd or an un-oxidized alloy should be carried out between membranes which have similar fluxes *in the absence of CO*. It has also been noted by Nguyen et al [2] that CO inhibition of a $Pd_{0.75}Ag_{0.23}$ alloy membrane increases as the thickness of the membrane decreases which is the same as the finding that the inhibiition increases with increase of flux. The earlier experiments

[1] were carried out employing mainly (H_2+C O) mixtures. Another method to compare the CO inhibition is to first expose the membranes to CO and then add the H_2 to initiate the permeation. With this pre-adsorbed approach, the effect of surface "blanketing" by CO during permeation is a smaller % as compared to its role with the employment of gaseous mixtures because the overall fraction of CO in the gas phase was much smaller in the pre-adsorbed approach. Because of its potential importance with regard to H_2 purification for use in fuel cells, a further investigation seems to be warranted not just with *Pd*–Al alloys but with other Pd alloys which can be IOed, e.g., *Pd*–Fe.

Internal oxidation, IO, occurs when an alloy, e.g., $Pd_{0.97}Al_{0.03}$, containing a minority metal, Al, which is more readily oxidizable than the majority metal, Pd, is heated in the atmosphere or in oxygen to temperatures greater than about 900 K. During internal oxidation the oxidation front penetrates from the outer surfaces inwardly [3] leading to the formation of nano-sized oxide precipitates within an essentially pure metal matrix within the oxidized layer. It has been shown that dissolved H is strongly trapped at the Pd/oxide internal interfaces and can be removed only by rather high temperature evacuation [4, 5], however, after these interface traps are filled by H, they play no further role in H diffusion within the IOed alloys [4].

In this work some H-permeation measurements will be carried out on IOed *Pd*–Al and IOed $(Pd_{0.77}Ag_{0.23})_{1-x}Al_x$ alloy membranes with and without pre-adsorbed CO. For the comparison of the effects of CO, measurements of the effect of pre-adsorbed CO will also be carried out on Pd and *Pd*–Ag alloys membranes which, of course, cannot be IOed. In addition, similar H permeation measurements will be carried out with IOed and un-oxidized *Pd*–Fe and *Pd*–Y alloy membranes.

Experimental

Alloys were prepared by arc–melting the pure elements together under argon. The resulting buttons were flipped and re-melted several times. They were then annealed *in vacuo* for 3 days at 1133 K and then rolled into foils of the appropriate thickness, i.e., ≈100 to 300 μm, for the diffusion membranes. The alloys form solid solutions over the range to be investigated. The area of the alloy membranes active for diffusion when mounted within the diffusion apparatus is 1.77 cm^2. The fluxes are determined from the small decreases of p_{up} with time as measured by an MKS electronic gauge where p_{up} is the upstream p_{H_2} and was usually chosen as the initial value of 50.7 kPa while

p_{down}=0 as described in earlier work [6, 7] on H permeation through Pd and Pd–Ag alloy membranes.

Fick's first law for diffusion in one dimension is given by

$$J = -D_H \left(\frac{dc_H}{dx}\right) \quad (1)$$

which, in the steady state for the above boundary conditions, reduces to

$$J = D_H c_{up}/d \quad (2)$$

where d is the membrane thickness and D_H is a composite diffusion constant reflecting the different degrees of concentration dependence of the diffusion constant within the membrane. D_H will be referred to as Fick's diffusion constant, c_{up} is the upstream H concentration and, in the steady state, dx in eq. (1) becomes d in eq. (2). The negative sign in eqn. (1) can be eliminated in eq (2) by defining dx→d as positive. The % decrease in flux due to CO will be calculated from $-((J - J_{CO})/J) \times 100\%$ where J and J_{CO} are the fluxes in the absence and presence of CO.

The alloys were IOed at elevated temperatures in the atmosphere. The % IO was determined from the weight gain. Upon IO, Pd–Al alloys form Al_2O_3 precipitates [4], *Pd*–Fe alloys form Fe_2O_3 precipitates [8] and *Pd*–Y alloys form Y_2O_3 precipitates [9]. For the IOed *Pd*–Al alloys nano-sized precipitates are seen with TEM but not many dislocations [10] whereas for IOed *Pd*–Fe alloys large dislocation densities were found [11]. TEM showed that the Y_2O_3 oxide precipitates formed after IO at 1100 K were from 10-30 nm in length and there was a low dislocation density [9].

For the inhibition studies, CO was introduced to the upstream side of the membranes allowing CO to be pre-adsorbed onto the upstream surface of the membrane at the temperature to be employed for the inhibition studies. A valve adjacent to the membrane enclosing a small volume, 3.0 cm^3, was then shut the remaining CO was evacuated and pure H_2 was introduced into the much greater volume, ≈600 or 1000 cm^3, at the desired p_{H_2}. The permeation was initiated by opening the valve separating the small and large volumes containing CO and the pure H_2, respectively. Under these conditions the fraction of CO in the gas phase during permeation was quite small, e.g., 0.006% for p_{up}=50.7 kPa when the volume containing the H_2 was 600 cm^3. The 600 and 1000 cm^3 volumes were employed for membranes which had relatively slow and fast permeation rates, respectively.

Results and Discussion

Pd and *Pd*–Al Alloys

Dependence of fluxes on (1/d)

If a plot of H flux versus (1/d) at a constant temperature and p_{up} is linear, then it follows from eq. (2) that the slow step is bulk diffusion through the membrane. For the apparatus to be employed in this research it has been previously shown that such a linear relationship obtains over a wide range of (1/d) values for pure Pd membranes [7]. Similar measurements are repeated here, however, in order to compare the results with measurements of the (1/d) dependence of the flux in the *presence* of pre-adsorbed CO. A linear relationship between J and (1/d) for Pd membranes in the absence of CO is shown in Figure 1 for the present results which again demonstrate that the slow step is bulk diffusion where c_{up} is determined by rapid equilibrium with p_{up}.

In the presence of pre-adsorbed CO there is no longer a linear relation between J and (1/d) (Fig. 1). The degree of CO inhibition is seen to depend on the flux in the absence of CO because the greater this flux, the greater the degree of inhibition, e.g., according to Figure 1 for J=18×10^{-7}(mol H/s)/cm^2 the percent decrease of flux due to CO is –61% and for J=6×10^{-7} it is –25%.

In the absence of CO, $c_{H,up}$ is the constant, equilibrium value determined by p_{up}=50.7 kPa and therefore the only variable determining the flux is (1/d) (eq. (2)). In the presence of pre-adsorbed CO, however, both (1/d) and $c_{H,up}$ are variables and the latter is smaller than its equilibrium value (Fig. 1). The initial $c_{H,up}$ values in the presence of pre-adsorbed CO can be estimated (Fig. 1) using eq. (2)

$$c_{H,up} = J_{CO}\ d/D_H. \tag{3}$$

where J_{CO} is the initial, steady state flux in the presence of pre-adsorbed CO as determined by extrapolation of the flux to t=0. Some calculated $c_{H,up}$ values are shown in Table 1 for Pd membranes at 423 K and 473 K. It is seen that in the presence of pre-adsorbed CO, $c_{H,up}$ decreases, as d decreases. For data at smaller 1/d values at these temperatures, the decrease of J is approximately linear and then it tends to level off at higher values of 1/d.

H fluxes are shown for the $Pd_{0.77}Ag_{0.23}$ alloy membrane in Figure 2 for both 423 and 523 K in the presence and absence of pre-adsorbed CO. In the absence of CO the flux is slightly greater at the lower temperature because of the greater H_2 solubility [6]. The dependence of J_{CO} on (1/d) at 423 K is especially noteworthy because J_{CO} is independent of (1/d) over the range of (1/d) values

Table 1: Calculated initial values of $c_{H,up}$ for Pd membranes in the absence and presence of pre-adsorbed CO (0.67 kPa) with p_{up}=50.6 kPa at 423 K.

423 K		
(1/d)/cm^{-1}	$c_{H,up}$/mol H/cm^3 at p_{CO}=0	$c_{H,up}$/mol H/cm^3 at p_{CO}=0.67 kPa
20.8	0.00288	0.00239
33.3	0.00288	0.00216
40.0	0.00288	0.00191
48.5	0.00288	0.0074
62.5	0.00288	0.00157
78.7	0.00288	0.00145
105.3	0.00288	0.00120
473 K		
(1/d)/cm^{-1}	p_{CO}=0	p_{CO}=0.67 kPa
21.1	0.00175	0.00171
26.3	0.00175	0.00163
31.3	0.00175	0.00156
40.0	0.00175	0.00152
57.5	0.00175	0.00146
71.4	0.00175	0.00137
109.9	0.00175	0.00108

investigated. In the region of constant J_{CO}, $c_{H,up}$ must be directly proportional to d according to eq. (3). At 423 K, J_{CO} must increase at smaller 1/d values than those measured in Figure 2 because when p_{CO}=0, the flux is significantly larger than the constant value.

At 423 K in the region for the $Pd_{0.77}Ag_{0.23}$ alloy membrane where J_{CO} is nearly constant with (1/d) (Fig. 2), examination of the time dependence of the J_{CO} at given 1/d values reveals that J_{CO} is nearly constant with time and, consequently, $c_{H,up}$, must be nearly constant with time or

$$\left(\frac{dc_{H,up}}{dt}\right)/A = 0 = c_1 - J_{CO} = c_1 - \frac{c_{H,up}D_H}{d} \tag{4}$$

where A is the area of the membrane and c_1 is the rate of H transfer from the gas phase to the up-stream side of the membrane. Under these conditions,

$$c_1 = J_{CO} \text{ and } c_{H,up} = d\ c_1/D_H. \tag{5}$$

In the region where J_{CO} is nearly constant with (1/d) (Fig. 2), the CO coverage must be significantly greater than its initial value at t=0 and therefore c_1 must also be smaller than its initial value (eq (5)).

For membranes at temperatures where J_{CO} is not constant with 1/d, $(dc_{H,up}/dt) < 0$ and therefore it follows from eq. (4) that $c_{H,up}$ will be larger than the value predicted by eqn (5).

The effect of pre-adsorbed CO on H permeation through $Pd_{0.77}Ag_{0.23}$ alloy membranes is similar to the effect of CO on Pd membranes as shown in Table 2 where two membranes are compared which have closely similar fluxes in the absence of CO. Although there appears to be a slightly greater effect of CO on the $Pd_{0.77}Ag_{0.23}$ alloy membrane, the differences are nearly within experimental error which demonstrates the reproducibility of these inhibitory effects of CO.

Fluxes in the presence and absence of pre-adsorbed CO.

The CO inhibition of H flux through IOed $Pd_{0.96}Al_{0.04}$ alloy membranes will be compared to the CO inhibition through Pd membranes rather than to un-oxidized $Pd_{0.96}Al_{0.04}$ alloy membranes because it proved to be more difficult to prepare un-oxidized alloys of different thicknesses with comparable fluxes as the IOed alloy membranes. It was found earlier that there is little difference between the CO inhibition of the un-oxidized *Pd*–Al alloy membranes and Pd membranes which have similar fluxes in the absence of CO [1] and it is seen in Table 2 that the inhibition by CO of H-flux through Pd and $Pd_{0.77}Ag_{0.23}$ alloys membranes is quite similar. The p_{H_2} boundary conditions of p_{up}=50.7 kPa and p_{down}=0 will be employed for the flux measurements in both the presence and absence of CO where the latter is pre-adsorbed in the absence of H_2 by exposure to p_{CO}=0.67 kPa at same the temperature as employed for the flux measurements.

Before presenting inhibition results using only pre-adsorbed CO, the inhibitory effects of pre-adsorbed CO and (H_2 + CO) mixtures will be compared. For inhibition by (H_2 + CO) mixtures, CO(0.67 kPa) and H_2(50.7 kPa) are mixed in the large volumes, 600 or 1000 cm^2, and then allowed to enter the membrane chamber to initiate the permeation studies. The total amount of CO in the gaseous volume exposed to the membrane is much larger for the (H_2 + CO) mixtures than for the pre-adsorbed CO.

Much of the work to be described here will be carried out with $Pd_{0.96}Al_{0.04}$ alloy membranes. Several different *Pd*–Al alloy compositions were employed earlier [1] but not specifically the $Pd_{0.96}Al_{0.04}$ alloy which has been chosen

because the Al concentration is great enough to show the effects of IO but small enough to preclude any surface oxidation.

Figure 3 shows comparisons at 423 K of CO inhibition of a Pd (180 μm) membrane and an IOed $Pd_{0.96}Al_{0.04}$ alloy membrane (128 μm) IOed at 953 K. It can be seen that their fluxes are quite similar before exposure to CO. The fluxes for the IOed $Pd_{0.96}Al_{0.04}$ and Pd membranes in Figure 3 have been adjusted to the fluxes at t=0 using: J(adjusted)/J(measured)=$\sqrt{p(t=0)/p(t)}$ where the p refers to p_{H_2}. It is seen for both the Pd and the IOed $Pd_{0.96}Al_{0.04}$ alloy membranes that the fluxes are more constant with time for the pre-adsorbed CO than for the mixture, indicating a larger role of "blanketing" of the surface by CO for the latter. The CO inhibition for the Pd membrane is seen to be greater for pre-adsorbed CO than for the gaseous mixture. The greater resistance towards CO inhibition of H permeation by the IOed $Pd_{0.96}Al_{0.04}$ alloy membrane as compared to the Pd membrane can be clearly seen in Figure 3 for both pre-adsorbed CO and for (H_2 + CO) mixtures.

In the following Figures and Tables, the fluxes have not been adjusted to reflect the small decreases of p_{up} with time of permeation as was done for the results in Figure 3 because the purpose of the research is the comparison of the relative effects of CO on IOed and un-oxidized membranes and this will not be significantly affected by small corrections to the fluxes due to decreases of p_{up} with time of permeation.

Following identical exposures to pre-adsorbed CO, it is shown in Figure 4 that the H flux (423 K) through the Pd membrane decreases by a factor of almost two compared to the flux through the IOed (10%) $Pd_{0.96}Al_{0.04}$ alloy membrane. Although both fluxes decrease with time (Fig. 4) the *differences* between the fluxes of the IOed and un-oxidized membranes are seen to be nearly constant with time. At 473 K (Fig 5) the degree of protection against CO inhibition by IO is not as great as at 423 K (Figs. 4) and it is also not as great at 523 K (Fig. 6), however, at both of these higher temperatures there are still greater decreases of flux due to CO for the Pd than for the IOed $Pd_{0.96}Al_{0.04}$ alloy membranes which have similar fluxes as Pd in the absence of CO.

Another series of comparison experiments were carried out with a 200 μm $Pd_{0.96}Al_{0.04}$ alloy membrane which was IOed to 57.8%; the Pd membrane used for comparison was 360 μm in thickness. The results at 423 K are shown in Figure 7 where it can be seen that the same conclusions hold for this alloy membrane which was IOed to a larger extent than the one shown in Figures 4-6 which was IOed 10%. The decreases of J due to CO are greater for both the Pd and IOed membranes shown in Figure 7 because of their faster rates,

however, the ratio of the decreases due to pre-adsorbed CO are similar to that in Figure 4, i.e., there is a factor of approximately 2× greater inhibition for Pd than for the IOed alloy membrane. Therefore a greater degree of IO does not significantly change the ratio of the decreases of J due to CO, i.e., the ratio (ΔJ (Pd)/ΔJ (IOed alloy)) is unchanged where ΔJ refers to the % decrease of J due to pre-adsorbed CO.

Table 3 shows results for a $Pd_{0.96}Al_{0.04}$ alloy membrane which was IOed to 6.8% as compared to a Pd membrane having a comparable flux in the absence of CO where it can be seen that the ratio (ΔJ (Pd)/ΔJ (IOed alloy)) is slightly larger than for the 10% IOed alloy.

Table 4 shows a tabulation of results for $Pd_{0.96}Al_{0.04}$ alloy membranes which have been IOed at different temperatures and also shown are results for a membrane whose thickness was reduced *after* IO. There is perhaps a slight increase in the inhibition due to CO as the % IO decreases but the effect is small as seen in Figures 4 and 7. The fluxes are somewhat faster after greater degrees of IO (953 K) because both D_H and the solubility are greater in the IOed portion, Pd, than in the un-oxidized portion and this may account for the small increases of CO inhibition with the extent of IO. It is clear that alloys which have been IOed at T>953 K, have a lesser resistance to CO than those IOed at a lower temperature and this is due to the larger oxide precipitates which form at elevated temperatures [3]. These larger precipitates are not as effective as the smaller ones resulting from the lower temperature IO [3] in protection against CO inhibition. The alloy which was IOed at 1093 K also has a large degree of inhibition and, after removal of some outer surface by treatment with abrasive paper, the inhibition did not change significantly.

Some results for a $Pd_{0.94}Al_{0.06}$ alloy IOed to 8.8% are shown in Table 5 compared with a Pd membrane with a similar CO-free flux. It can be seen that the ratio: (ΔJ (Pd)/ΔJ (IOed alloy)) at 423 K is about two which is similar to that found for an IOed $Pd_{0.96}Al_{0.04}$ alloy at the same conditions of p_{up} and p_{CO} indicating that the specific % Al in this range of Al contents is not important. Al contents greater than about 10% have been avoided, however, because they will undergo not only IO but also external oxidization [3].

$(Pd_{0.77}Ag_{0.23})_{0.96}Al_{0.04}$ Alloys

The $Pd_{0.77}Ag_{0.23}$ alloy is the most frequently employed membrane for H_2 purification because of its large H permeability and because it does not form a hydride phase at ≥300 K. If this binary alloy is alloyed with small amounts

of Al, the resulting alloy can be IOed which should give it a greater resistance to CO and possibly to other gaseous poisons. Results are shown in Tables 6-8 where it can be seen that the fluxes are greater for these than for the $Pd_{0.96}Al_{0.04}$ alloy membrane because of the greater permeability of the $Pd_{0.77}Ag_{0.23}$ alloy. The inhibition by CO of the IOed $(Pd_{0.77}Ag_{0.23})_{0.96}Al_{0.04}$ alloy is compared to the $Pd_{0.77}Ag_{0.23}$ alloy rather than to pure Pd because it was not possible in some cases, to obtain the appropriately large fluxes with Pd. Although the CO inhibition of the IOed $(Pd_{0.77}Ag_{0.23})_{0.96}Al_{0.04}$ alloy is seen to be significant (Tables 7, 8), it is still smaller than that for the $Pd_{0.77}Ag_{0.23}$ alloy at the temperatures measured, This indicates that it may be useful to employ IOed $(Pd_{0.77}Ag_{0.23})_{1-x}Al_x$ alloy membranes for practical H_2 purification under conditions where CO can be a factor, e.g., in reformation gas mixtures.

Table 2: J in arbitrary units for $Pd_{0.77}Ag_{0.23}$ Alloy and Pd Membranes at p_{H_2}=50.7 kPa with pre-adsorbed p_{CO}=0.67.

	J as a function of perm. time, 523 K					
$Pd_{0.77}Ag_{0.23}$ **Alloy**	0–5m	5–10m	10–15m	15–20m	20–25m	25-30m
pure H_2	1.84	1.80	1.76	1.72	1.68	1.64
pre-ads. CO	1.48	1.30	1.12	1.00	0.88	0.80
% red.	–19.6%	–27.8%	–37.1%	–49.5%	–56.7%	–62.4%
	J as a function of perm. time, 523 K					
pure Pd	0–5m	5–10m	10–15m	15–20m	20–25m	25-30m
pure H_2	1.92	1.90	1.88	1.84	1.80	1.78
pre-ads. CO	1.56	1.40	1.20	1.06	0.96	0.88
% red.	–18.8%	–26.3%	–36.2%	–42.4%	–46.7%	–50.6 %
	J as a function of perm. time, 473 K					
$Pd_{0.77}Ag_{0.23}$ **Alloy**	0–5m	5–10m	10–15m	15–20m	20–25m	25-30m
pure H_2	3.08	3.00	2.92	2.80	2.72	2.64
pre-ads. CO	1.40	1.16	0.96	0.84	0.76	0.68
% red.	–48.7%	–59.3%	–65.1%	–68.6%	–72.1%	–74.2 %
	J as a function of perm. time, 473 K					
pure Pd	0–5m	5–10m	10–15m	15–20m	20–25m	25-30m
pure H_2	3.08	3.00	2.94	2.86	2.80	2.72
pre-ads. CO	1.60	1.24	1.04	0.88	0.80	0.72
% red.	–48.1%	–58.7%	–64.6%	–69.2%	–71.4%	–73.5%
	J as a function of perm. time, 423 K					
$Pd_{0.77}Ag_{0.23}$ Alloy	0–5m	5–10m	10–15m	15–20m	20–25m	25-30m
pure H_2	2.00	1.88	1.84	1.80	1.76	1.72
pre-ads. CO	0.52	0.52	0.52	0.52	0.48	0.48
% red.	–74.0%	–72.3%	–71.7%	–71.1%	–72.7%	–72.1 %
	J as a function of perm. time, 423 K					
pure Pd	0–5m	5–10m	10–15m	15–20m	20–25m	25-30m
pure H_2	2.08	2.04	2.00	2.00	1.96	1.92
pre-ads. CO	0.56	0.54	0.54	0.52	0.52	0.48
% red.	–73.1%	–73.5%	–73.0 %	–74.0%	–73.5%	–75.0%

Table 3: J/ 10^{-6}mol H/cm^2-s at 423 K for a $Pd_{0.96}Al_{0.04}$ Alloy (100 μm) IOed at 953 K to 6.8% and Pd (160 μm), p_{H_2}=50.7 kPa and p_{CO}=0.67 kPa.

	J as a function of perm. time					
alloy (IOed)	0–5m	5–10m	10–15m	15–20m	20–25m	25-30m
pure H_2	0.94	0.92	0.89	0.88	0.88	0.86
pre-ads. CO	0.78	0.76	0.72	0.69	0.68	0.66
% red.	–17.0%	–17.4%	–19.1%	–21.6%	–22.7%	–23.2%
	J as a function of perm. time					
pure Pd	0–5m	5–10m	10–15m	15–20m	20–25m	25-30m
pure H_2	0.92	0.89	0.88	0.88	0.86	0.84
pre-ads. CO	0.55	0.53	0.52	0.51	0.50	0.48
% red.	–40.2%	–40.4%	–40.9 %	–41.8%	–41.8%	–42.8 %

Table 4: Initial Fluxes at 423 K through $Pd_{0.96}Al_{0.04}$ Alloy Membranes IOed at various temperatures, p_{H_2}(up)=50.7 kPa and their Susceptibility to Pre-adsorbed CO (0.67 kPa CO) as compared to Pd membranes with comparable CO-free fluxes.

IO Temp.	%IO	J/10^{-6}mol H /cm^2-s CO-free	J decrease %
953 K	6.8	1.02	–17.1
953 K	9.2	1.05	–21.5
953 K	33.7	1.15	–23.2
953 K	57.8	1.32	–22.5
1093 K	57.3	1.27	–60.8
1093 K	*	1.34	–60.8
1273 K	57.0	1.14	-62.2

*remove some surface of the 57.3% IOed alloy with emory paper.

Table 5: Fluxes at 423 K using p_{up}=50.7 kPa through a Pd and a $Pd_{0.94}Al_{0.06}$ Alloy membrane IOed (8.8%) with and without pre-adsorbed CO (0.67 kPa)

	$J/10^{-6}$mol H /cm^2-s					
	Pd(160μm)			IOed alloy(80μm), IOed 8.8%		
t/m	p_{CO}=0	p_{CO}=0.66 kPa	% red.	p_{CO}=0	p_{CO}=0.66 kPa	% red.
0-5	0.92	0.55	–40.5	0.91	0.72	–19.4
5-10	0.89	0.53	–40.3	0.89	0.68	–21.4
10-15	0.88	0.52	–40.9	0.88	0.66	– 23.2
15-20	0.88	0.51	–42.3	0.87	0.65	– 24.6
20-25	0.86	0.50	–42.0	0.86	0.62	– 27.5
25-30	0.84	0.48	–42.6	0.84	0.60	– 29.4

Table 6: Fluxes in arbitrary units (423 K) using p_{up}=50.7 kPa through a $Pd_{0.77}Ag_{0.23}$ (356μm) membrane and a $(Pd_{0.77}Ag_{0.23})_{0.96}Al_{0.04}$ (102μm) membrane IOed at 953 K to 12.6%,

	J (arb. units) as a function of time					
IOed ternary alloy	0–5m	5–10m	10–15m	15–20m	20–25m	25-30m
H_2	1.86	1.82	1.78	1.76	1.74	1.70
H_2+pre-ads CO	0.90	0.80	0.72	0.66	0.60	0.54
% red.	–51.6%	–56.0%	–59.6%	–62.5%	–65.5%	–68.2%
	J (arb. units) as a function of time					
binary alloy	0–5m	5–10m	10–15m	15–20m	20–25m	25-30m
H_2	2.00	1.88	1.84	1.80	1.76	1.72
H_2+pre-ads CO	0.44	0.44	0.40	0.40	0.40	0.38
% red.	–78.0%	–76.6%	–78.3 %	–77.8%	–77.3%	–77.9 %

Table 7: Fluxes in arbitrary units 473 K using p_{up}=50.7 kPa through a $Pd_{0.77}Ag_{0.23}$(300μm) and a $(Pd_{0.77}Ag_{0.23})_{0.96}Al_{0.04}$(102$\mu$m) alloy membrane IOed at 953 K to 12.6%, p_{H_2}=50.7 kPa

	J (arb. units)as a function of time					
IOed ternary alloy	0–5m	5–10m	10–15m	15–20m	20–25m	25-30m
H_2	2.18	2.14	2.10	2.06	2.02	1.97
H_2+pre-ads CO	1.60	1.36	1.14	1.00	0.90	0.80
% red.	–26.6%	–36.4%	–45.1%	–51.5%	–54.5%	–59.4%
	J (arb. units) as a function of time					
unox. binary alloy	0–5m	5–10m	10–15m	15–20m	20–25m	25-30m
H_2	2.28	2.22	2.18	2.12	2.08	2.04
H_2+pre-ads CO	1.20	1.00	0.84	0.74	0.66	0.60
% red.	–47.4%	–55.0%	–61.5 %	–65.1%	–68.3%	–70.6 %

Table 8: Fluxes/mol H/cm^2-s (523 K) using p_{up}=50.7 kPa through a $Pd_{0.77}Ag_{0.23}$(265μm) and a $(Pd_{0.77}Ag_{0.23})_{0.96}Al_{0.04}$ (102μm) alloy membrane IOed at 953 K to 12.6%

	J (arb. units) as a function of t					
IOed ternary	0–5m	5–10m	10–15m	15–20m	20–25m	25-30m
H_2	2.56	2.50	2.44	2.38	2.32	2.26
H_2+pre-ads CO	1.88	1.50	1.24	1.06	0.90	0.80
% red.	–26.6%	–40.0%	–49.2%	–55.5%	–61.2%	–64.6%
	J (arb. units) as a function of t					
unox. binary	0–5m	5–10m	10–15m	15–20m	20–25m	25-30m
H_2	2.56	2.52	2.46	2.40	2.36	2.28
H_2 + pre-ads CO	1.72	1.40	1.20	1.04	0.88	0.76
% red.	–32.8%	–44.4%	–51.2 %	–56.7%	–62.7%	–66.7 %

Effect of CO on ($Pd_{1-x}Fe_x$) Alloy Membranes

It was of interest to determine whether or not $Pd_{1-x}Fe_x$ alloy membranes also exhibit increased resistance to CO after IO because it has been found that these can be IOed to high % IO without as much cracking as the *Pd*–Al alloys at similar % IO [14]. This has the advantage that *Pd*-Fe or $(Pd_{0.77}Ag_{0.23})_{1-x}Fe_x$ alloy membranes can be completely IOed leading to Pd or $Pd_{0.77}Ag_{0.23}$ membranes with much larger permeabilities than the un-oxidized membranes. Figure 8 shows a plot of J versus (1/d) for $Pd_{0.963}Fe_{0.037}$ alloy membranes with different thicknesses (423 K) with and without pre-adsorbed CO. A quite linear relation is seen between J and (1/d) for the IOed alloy in the absence of CO indicating bulk diffusion as the slow step but, in the presence of CO, the relationship is non-linear indicating that a surface step has become a contributor, i.e., the behavior is very similar to Pd (Fig. 1) and to $Pd_{0.77}Ag_{0.23}$ alloy membranes (Fig. 2).

A $Pd_{0.963}Fe_{0.037}$ alloy was IOed to about 5% and typical results before and after exposure to pre-adsorbed CO are shown in Figure 9 at 423 K where it can be seen that there is a significantly greater effect of CO on the Pd membrane than on the IOed alloy membrane. Similar results are found at 473 and 523 K, and, as for the IOed *Pd*–Al alloy membranes, the effect of IO is not as great at the higher temperatures. The ratio: (ΔJ (Pd)/ΔJ (IOed alloy)) is $\approx$2 at 423 K which is the about same as for the IOed $Pd_{0.96}Al_{0.04}$ membrane at this temperature (Fig. 3). Thus completely IOed *Pd*–Fe alloy or $(Pd_{0.77}Ag_{0.23})_{1-x}Fe_x$ membranes may be promising as H_2 purification membranes since their permeabilities will be high especially for the latter.

Table 9 shows results at 423 K for IOed $Pd_{0.927}Fe_{0.073}$ alloy membranes as compared to pure Pd. The results are similar to those found for the $Pd_{0.963}Fe_{0.037}$ alloy membrane, i.e., there is a markedly greater resistance to CO for the IOed alloy as compared to pure Pd.

Table 9: J(arb. units) at 423 K for Pd and a series of IOed $Pd_{0.927}Fe_{0.073}$ alloy membranes IOed (10-15%), p_{up}=50.7 kPa and CO=0.67 kPa in the mixture and in the small volume for pre-adsorbed CO. The 2nd, 3rd and 5th and 6th columns are the % decrease in J.

IOed $Pd_{0.927}Fe_{0.073}$			Pd		
J(H_2)	(H_2 +CO)	pre-ads. CO	J (H_2)	(H_2 +CO)	pre-ads. CO
0.84	0	–4.8	0.84	–3.9	–14.3
0.98	–2.0	–8.3	0.98	–6.2	–24.5
1.16	–3.5	– 12.1	1.06	–7.6	–28.9
1.56	–5.1	–15.4	1.48	–12.2	–40.5
2.28	–5.1	–15.4	1.94	–15.5	–45.4

Effect of CO on ($Pd_{1-x}Y_x$) Alloy Membranes

Pd–Y alloy membranes have been proposed for H_2 purification because of their large H permeabilities [18]. For this reason it was of interest to learn whether or not partially IOed ($Pd_{1-x}Y_x$) alloy membranes have a greater resistance to CO than do un-oxidized alloys which have similar permeabilities in the absence of CO. Since these alloys have large permeabilities, it was decided to compare their permeabilities after IO to *Pd*–Ag alloy membranes which also have large permeabilities.

Some typical results are seen in Figure 10 where the CO-free fluxes are similar for the two alloys but it can be seen that the IO does not protect an IOed (5%) $Pd_{0.956}Y_{0.044}$ alloy membrane significantly. It is not known why this is the case because the alloy was also IOed at 953 K, i.e., the same temperature employed for *Pd*–Al and *Pd* –Fe alloy membranes, which leads leads to small oxide precipitates in all of these alloys. There was no obvious difference in the micro-structures observable from TEM between the IOed alloys which would lead to a difference in their behavior towards CO. This lack of resistance to CO was also found for other Pd–Y alloy membranes.

Origin of the Increased Resistance to CO after IO.

Generally after IO, SEM micrographs reveal Pd nodules on the surface along with some oxide precipitates [12]. A typical SEM photomicrograph after IO of a $Pd_{0.926}Fe_{0.074}$ alloy (1073 K) shows thermal grooves and Pd nodules. In some SEM photos, oxide precipitates are also seen. The surfaces are quite rough after IO compared to the un-oxidized alloys. There are no obvious clues from SEM or TEM concerning the greater resistance to CO inhibition of the IOed *Pd*–Fe and –Al alloys as compared to IOed *Pd*–Y alloy membranes.

Conclusions

It is shown that IOed *Pd*-Al and *Pd*-Fe alloy H permeation membranes have a greater resistance to pre-adsorbed CO than do un-oxidized alloys with similar H fluxes in the absence of CO. Partial IO is a very simple procedure which can be readily employed and may prove to be useful for H purification membranes under conditions where CO may be an impurity, e.g., in gaseous mixtures resulting from reformation of hydrocarbons. It is shown that the inhibition effect of CO is greatest at lower temperatures, e.g., 423 K, and protection

against CO by IO is also greatest at lower temperatures. It should also be pointed out that permeation of H through $Pd_{0.77}Ag_{0.23}$ alloy membranes is similar at 423 to 523 K for p_{up}=50.6 kPa because, although D_H decreases with decrease of temperature, the solubility increases significantly [6]. There may be advantages in employing lower temperature H purification, e.g., poisoning by H_2S may be less significant because its dissociation may not occur at lower temperatures. Long term exposures to CO have not been carried out and this may be needed before the actual employment of IOed Pd-based membranes.

Acknowledgements

This work was supported by Westinghouse Savannah River Company under U.S. Department of Energy Contract Number DE-AC09-96SR185000.

References

[1] D. Wang, T. Flanagan, K. Shanahan, *J. Membrane Sci.,* **253** (2005) 165.

[2] T. Nguyen, S. Mori, M. Suzuki, *Chem. Eng. J.,* **155** (2009) 55.

[3] J. Meijering, *Adv. Mat. Research,* **5** (1971) 1.

[4] X. Huang, W. Mader, R. Kirchheim, *Acta metall. mater.,* **39** (1991) 893.

[5] D. Wang, H. Noh, S. Luo, T. Flanagan, J. Clewley, R. Balasubramaniam, *J. Alloys Compounds,* **339** (2002) 76.

[6] D. Wang, T. Flanagan, K. Shanahan, *J. Phys. Chem.B,* **112** (2008) 1135.

[7] T. Flanagan, D. Wang, K. Shanahan, *J. Membrane Sci.,***306** (2007) 66.

[8] J. Gegner, *PhD Thesis, University Stuttgart*, 1995.

[9] W. Zhang, S. Luo, D. Wang, T. Flanagan, R. Balasubramaniam, *J. Alloys Compounds,* **330-332** (2002) 607.

[10] R. Balasubramaniam, H. Noh, T. Flanagan, Y. Sakamoto, *acta Mater.,* **45** (1997) 1725.

[11] D. Wang, T. Flanagan R. Balasubramaniam, *J. Alloys Compounds,*, **356-357** (2003) 3.

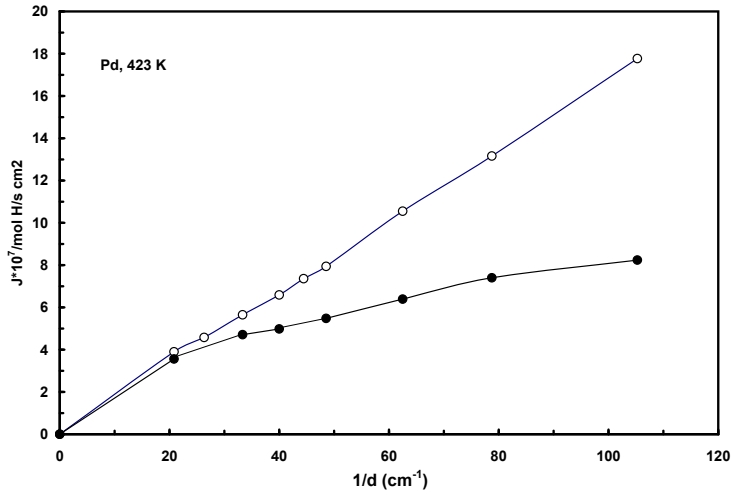

Figure 1: H fluxes through Pd membranes plotted against 1/d in the presence and absence of pre-adsorbed CO (0.66 kPa) with p_{up}=50.7 kPa. ○, H_2 only p_{H_2} =50.7 kPa; ●, flux in the presence of pre-adsorbed CO at 423 K.

[12] R. Balasubramaniam, R. Kirchheim, D. Wang, T. Flanagan, *J. Alloys Compounds,* **293-295** (1999) 306.

[13] Y. Sakamoto, F. Chen, M. Ura, T. Flanagan, *Ber. Bunsenges Physik. Chem.,***99** (1995) 807.

[14] T. Flanagan, D. Wang, *J. Alloys Compounds*, **488** (2010) 72.

[15] W. Zhang, S. Luo, T. Flanagan, *J. Alloys Compounds*, **291-295** (1999) 1.

[16] T. Flanagan, G. Gross, J. Clewley, *2nd Int. Congress on Hydrogen in Metals,* Paris, France, 6-11, VI (1977).

[17] E. Wicke, H. Brodowsky, *Hydrogen in Metals, II*, G. Alefeld, J. Völkl, eds., Springer-Verlag, 1978.

[18] D. Hughes, J. Evans, I. Harris, *J. Less-Common Mets.,* **76** (1980) 119.

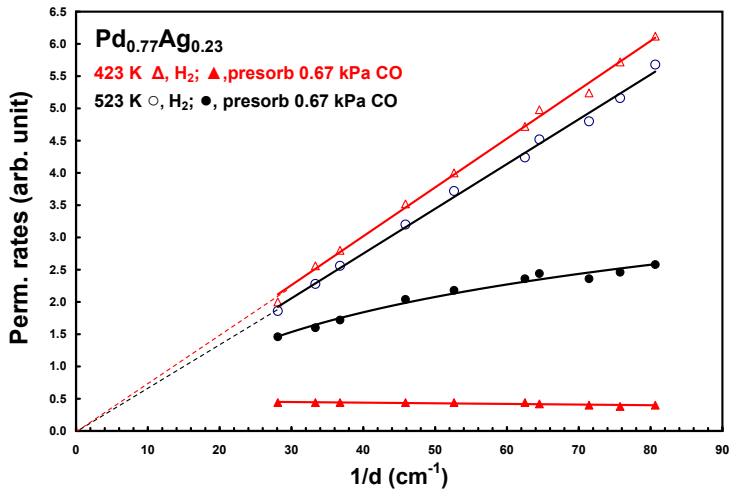

Figure 2: Fluxes through $Pd_{0.77}Ag_{0.23}$ alloy membranes plotted against 1/d in the presence and absence of pre-adsorbed CO (0.66 kPa) with p_{up}=50.7 kPa. △, flux in absence of CO at 423 K; ▲, flux in the presence of CO at 423 K; ◯, flux in the absence of CO at 523 K; ●, flux in the presence of CO at 523 K.

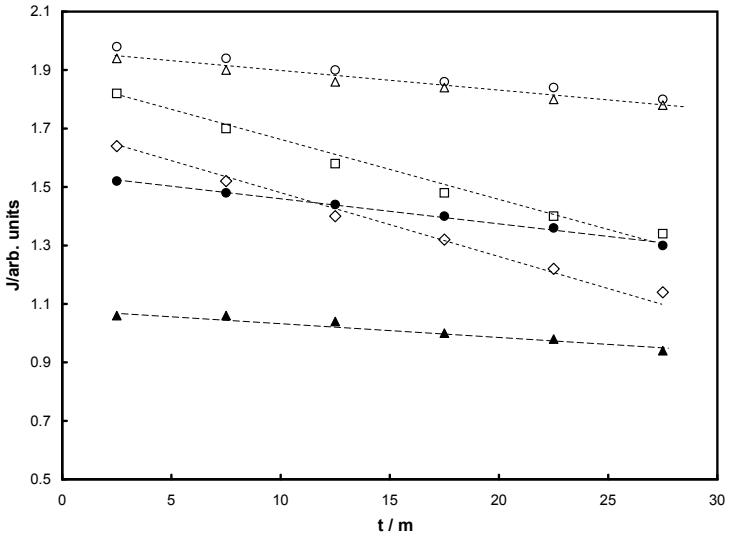

Figure 3: Plot showing H fluxes in arbitrary units against time with p_{up}=50.7 kPa (423 K) through Pd and through an IOed $Pd_{0.96}Al_{0.04}$ membrane in the absence of CO and in the presence of (H_2 + CO) mixtures and in the presence of pre-adsorbed CO (0.67 kPa). △, Pd membrane in the absence of CO; ○, IOed $Pd_{0.96}Al_{0.04}$ membrane in the absence of CO; □, IOed $Pd_{0.96}Al_{0.04}$ membrane in the presence of (H_2 + CO) mixture; ◇, Pd membrane in the presence of a (H_2 + CO) mixture; ●, IOed $Pd_{0.96}Al_{0.04}$ alloy membrane in the presence of pre-adsorbed CO; ▲, Pd membrane in the presence of pre-adsorbed CO

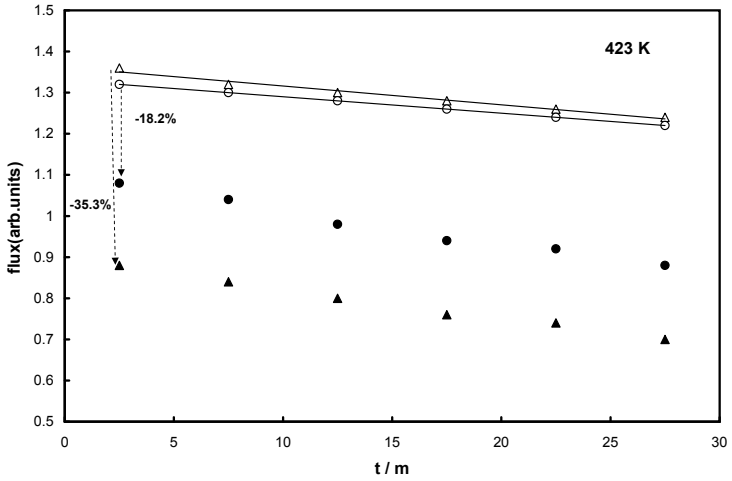

Figure 4: H flux in arbitrary units as a function of time for Pd and IOed (10%) $Pd_{0.96}Al_{0.04}$ membranes (423 K). △, Pd in the absence of CO; ▲, Pd in the presence of pre-adsorbed CO; ○, IOed $Pd_{0.96}Al_{0.04}$ in the absence of CO; ●, IOed $Pd_{0.96}Al_{0.04}$ in the presence of pre-adsorbed CO.

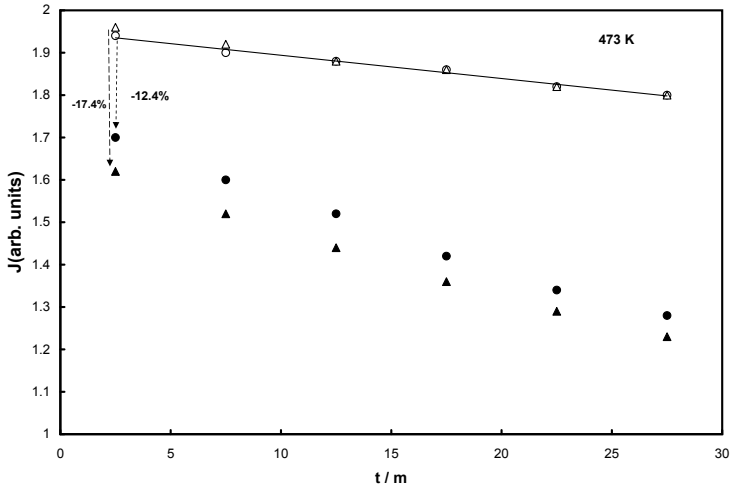

Figure 5: H flux in arbitrary units as a function of time for Pd and IOed (10%) $Pd_{0.96}Al_{0.04}$ membranes (473 K). △, Pd in the absence of CO; ▲, Pd in the presence of pre-adsorbed CO; ○, IOed $Pd_{0.96}Al_{0.04}$ in the absence of CO; ●, IOed $Pd_{0.96}Al_{0.04}$ in the presence of pre-adsorbed CO.

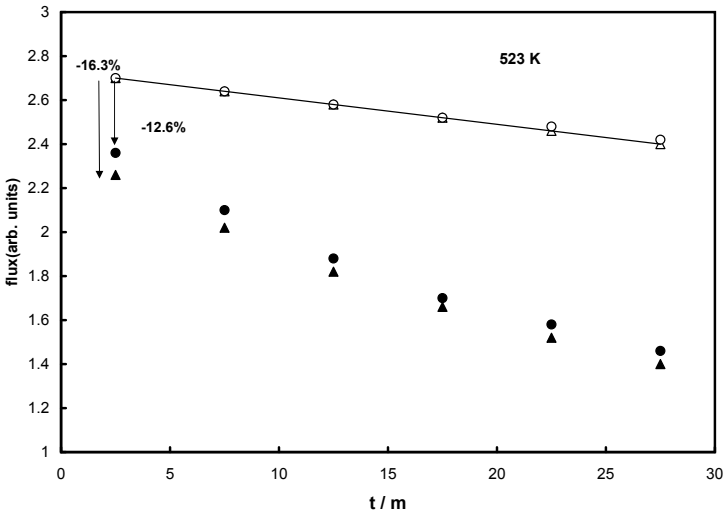

Figure 6: H flux as a function of time for Pd and IOed (10%) $Pd_{0.96}Al_{0.04}$ membranes plotted as flux in arbitrary units (523 K). △, Pd in the absence of CO; ▲, Pd in the presence of pre-adsorbed CO; ○, IOed $Pd_{0.96}Al_{0.04}$ in the absence of CO; ●, IOed $Pd_{0.96}Al_{0.04}$ in the presence of pre-adsorbed CO.

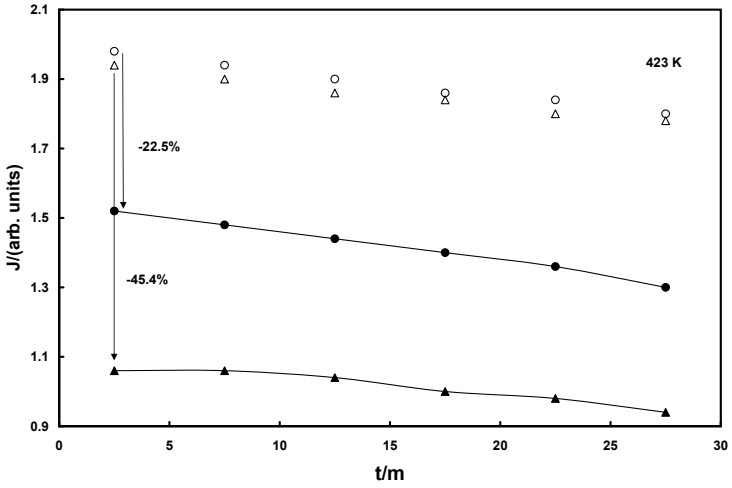

Figure 7: H flux in arbitrary units as a function of time (423 K) for Pd and a $Pd_{0.96}Al_{0.04}$ alloy membrane IOed to 57.8%. △, Pd in the absence of CO; ▲, Pd in the presence of pre-adsorbed CO; ○, IOed $Pd_{0.96}Al_{0.04}$ in the absence of CO; ●, IOed $Pd_{0.96}Al_{0.04}$ in the presence of pre-adsorbed CO.

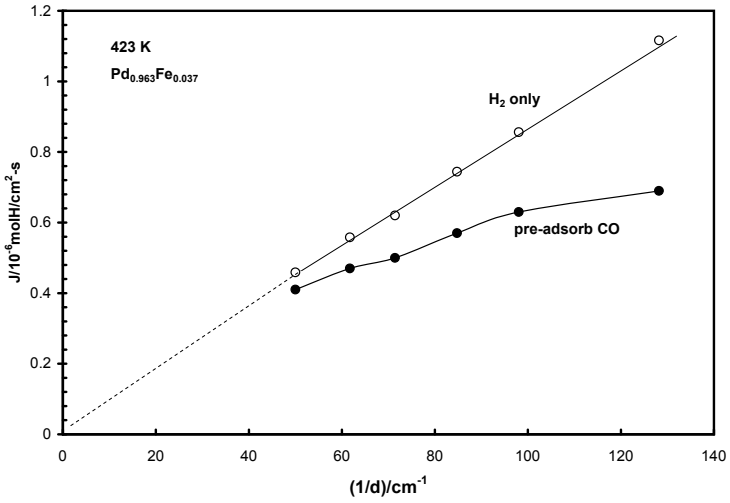

Figure 8: Plot showing the flux at p_{up}=50.7 kPa against 1/d through IOed $Pd_{0.963}Fe_{0.037}$ alloy membranes in the presence and absence of pre-adsorbed CO (423 K). ○, H_2 only; ●, pre-adsorbed CO.

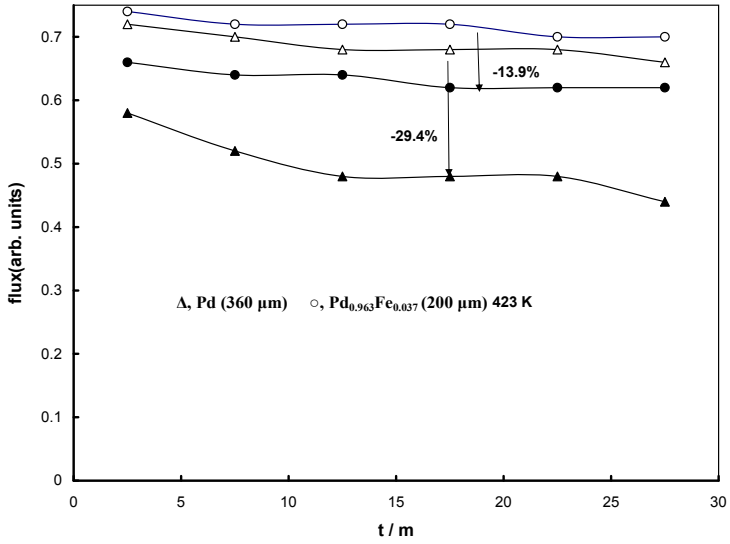

Figure 9: Decrease of flux of Pd and an IOed $Pd_{0.963}Fe_{0.037}$ membrane plotted as flux in arbitrary units against permeation time at 423 K. ○, IOed $Pd_{0.963}Fe_{0.037}$ in the absence of CO; ●, $Pd_{0.963}Fe_{0.037}$ in the presence of pre-adsorbed CO; △, Pd in the absence of CO; ▲, Pd in the presence of pre-adsorbed CO.

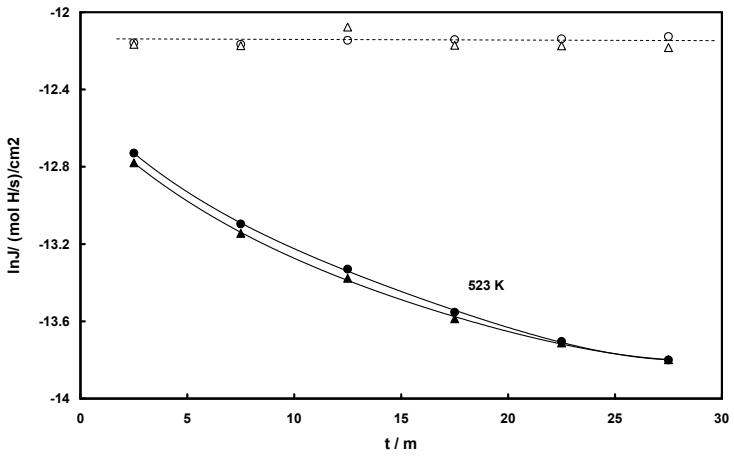

Figure 10: Decrease of ln J at 523 K of a IOed (10%) $Pd_{0.97}Y_{0.03}$ alloy membrane and an un-oxidized $Pd_{0.77}Ag_{0.23}$ alloy membrane against permeation time (523 K). ○, IOed $Pd_{0.97}Y_{0.03}$ alloy in the absence of CO; ●, IOed $Pd_{0.97}Y_{0.03}$ alloy in the presence of CO; △, $Pd_{0.77}Ag_{0.23}$ alloy in the absence of CO; ▲, $Pd_{0.77}Ag_{0.23}$ alloy in the presence of pre-adsorbed CO.